

# Quantum Monte Carlo study of molecular polarization and antiferroelectric ordering in squaric acid crystals

Hiroaki Ishizuka and Yukitoshi Motome

*Department of Applied Physics, University of Tokyo, Tokyo 113-8656, Japan*Nobuo Furukawa<sup>1,2</sup> and Sei Suzuki<sup>1</sup><sup>1</sup>*Department of Physics and Mathematics, Aoyama Gakuin University, Kanagawa 252-5258, Japan*<sup>2</sup>*Multiferroics Project, ERATO, Japan Science and Technology Agency (JST), c/o Department of Applied Physics, University of Tokyo, Tokyo 113-8656, Japan*

(Received 16 March 2011; revised manuscript received 19 May 2011; published 26 August 2011)

Effects of geometrical frustration and quantum fluctuation are theoretically investigated for the proton ordering in a quasi-two-dimensional hydrogen-bonded system, namely a squaric acid crystal. We elucidate the phase diagram for an effective model, the transverse-field Ising model on a frustrated checkerboard lattice, by using quantum Monte Carlo simulation. A crossover to a liquidlike paraelectric state with well-developed molecular polarizations is identified, distinguishably from long-range ordering. The emergence of long-range order from the liquidlike state exhibits peculiar aspects originating from the lifting of quasimacroscopic degeneracy, such as colossal enhancement of the transition temperature and a vanishingly small anomaly in the specific heat.

DOI: [10.1103/PhysRevB.84.064120](https://doi.org/10.1103/PhysRevB.84.064120)

PACS number(s): 77.80.-e, 75.10.Jm, 75.40.Mg, 77.84.Fa

## I. INTRODUCTION

Proton ordering in hydrogen-bonded systems has long been one of the central topics in condensed-matter physics. Each proton is in a double-minimum potential on the hydrogen bond, and spatial correlations among the proton configurations strongly affect macroscopic properties of hydrogen-bonded crystals. A famous example is the “ice-rule” configuration of protons and its relation to the residual entropy in water ice.<sup>1,2</sup> Another example is the ferroelectricity due to the proton ordering in  $\text{KH}_2\text{PO}_4$ .<sup>3-5</sup> Electronic polarization emerging from proton ordering has been studied extensively with an emphasis on both the fundamental physics and the application to electronic devices.<sup>6,7</sup>

Here, we focus on one such hydrogen-bonded material, namely squaric acid crystal  $\text{H}_2\text{C}_4\text{O}_4$  ( $\text{H}_2\text{SQ}$ ).  $\text{H}_2\text{SQ}$  is a quasi-two-dimensional (2D) molecular solid. In each 2D layer, squaric acid molecules form a network of hydrogen bonds, as shown in Fig. 1(a).<sup>8</sup> A particular configuration of protons induces a polarization in each molecule, and an ordering of the polarizations can lead to ferroelectricity. In fact,  $\text{H}_2\text{SQ}$  exhibits antiferroelectricity below  $T_c = 375$  K, which is driven by the 2D ferroelectric ordering with interlayer antiferroelectric coupling.<sup>9</sup>

$\text{H}_2\text{SQ}$  has two striking aspects. One is the local constraint on the proton positions similar to the ice rule in water ice. Each molecule has four hydrogen bonds; two out of four protons come close to the  $\text{C}_4\text{O}_4$  unit and the other two are far. The local constraint alone is not sufficient to determine a unique ground state and brings about a macroscopic degeneracy, as seen in water ice;  $\text{H}_2\text{SQ}$  has geometrical frustration in nature.

The other aspect is the effect of quantum tunneling of protons. In general, the external pressure increases the tunneling rate of protons between two potential minima, which reduces local polarizations, and consequently suppresses the ferroelectricity. Indeed, in  $\text{H}_2\text{SQ}$ ,  $T_c$  is sup-

pressed with increasing pressure. A peculiar intermediate state, however, appears before the polarization is lost in each molecule: the macroscopic polarization vanishes while the polarization in each molecule is retained.<sup>10</sup> Consequently, a quantum paraelectric state is realized in the low-temperature limit.

There have been many theoretical studies for the antiferroelectric transition in  $\text{H}_2\text{SQ}$ . The local constraint and associated frustration were considered on the basis of vertex models or frustrated pseudospin models.<sup>11-14</sup> The coupling between pseudospins and phonons was also studied.<sup>15-17</sup> Most of the studies, however, were limited at the mean-field level, and the effect of geometrical frustration has not been fully clarified yet. In particular, quantum fluctuation under the geometrical frustration, which is presumably important for understanding the quantum paraelectricity under pressure, has not been seriously considered so far.

In the present study, we investigate an effective model for  $\text{H}_2\text{SQ}$ , a 2D checkerboard-lattice Ising model with transverse field that corresponds to the application of external pressure. With a sophisticated quantum Monte Carlo (QMC) method, we map out the numerically exact phase diagram. We identify a liquidlike state intervening between the ferroelectric phase and the paraelectric phase. In the intermediate state, molecular polarizations are well retained by ice-rule-type local correlations, but they are globally disordered. The peculiar nature of transition from the intermediate state to ferroelectric phase is discussed.

The organization of this paper is as follows. In Sec. II, we introduce models and methods. After introducing the pseudospin model in Sec. II A, we describe the numerical method and the definition of the observables in Secs. II B and II C, respectively. The results of calculation are presented in Sec. III. The temperature dependence of observables is given in Sec. III A and the phase diagram in Sec. III B. Discussions

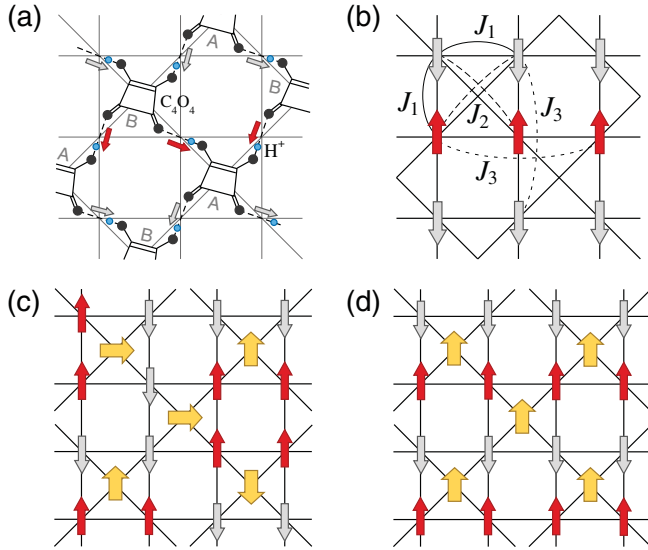


FIG. 1. (Color online) (a) Schematic picture of a layer of H<sub>2</sub>SQ molecules. The dashed lines represent hydrogen bonds connecting C<sub>4</sub>O<sub>4</sub> units, and small circles on the bonds show protons. (b) Pseudospin representation of the proton displacement in (a).  $J_1$ ,  $J_2$ , and  $J_3$  denote the interactions in Eq. (1). (c) An example of intermediate liquidlike states in which every molecule bears a polarization but the system is globally disordered. (d) A ferroelectrically ordered state. In (c) and (d), the bold arrows in the center of the plaquettes represent the molecular polarizations. See the text for details.

on our results with the previous studies are elaborated in Sec. IV. Section V is devoted to a summary.

## II. MODEL AND METHOD

### A. Pseudospin model

We consider here a pseudospin model for H<sub>2</sub>SQ following the previous studies.<sup>13,14</sup> In the pseudospin model, proton displacements in a plane of the bipartite square lattice of H<sub>2</sub>SQ molecules [Fig. 1(a)] are represented by the  $z$  component of pseudospins as  $\sigma_i^z = \pm 1$  [Fig. 1(b)].<sup>4,5</sup> Here the appropriate signs are assigned so that protons belonging to  $A(B)$ -sublattice H<sub>2</sub>SQ molecules correspond to the up (down) spins. The local constraint similar to the ice rule in water ice<sup>1,2</sup> (two out of four protons are close and the other two are far) is taken into account by the antiferromagnetic interactions between nearest neighbors,  $J_1$ , and crisscrossing next-nearest neighbors,  $J_2$ , on the checkerboard lattice.<sup>13,14</sup> When  $J_1 = J_2$ , the model is a 2D variant of the spin-ice model,<sup>18,19</sup> in which sixfold degeneracy in each plaquette results in a macroscopic number of energetically degenerate ground states  $\sim 1.5^N$ . In the present case, we take  $J_2 > J_1$  since two closer protons favor an edge of the C<sub>4</sub>O<sub>4</sub> square, not a diagonal.<sup>13,14</sup>  $J_2$  larger than  $J_1$  partially lifts the degeneracy, but the ground-state degeneracy still remains: all configurations with different stacking of antiferromagnetic 1D diagonal chains, exemplified in Figs. 1(c) and 1(d), give the same lowest energy. The degeneracy is reduced but still quasimacroscopic, i.e.,  $4^{\sqrt{N}}$ . Hence, the present  $J_1$ - $J_2$  model does not show any long-range order down to zero  $T$ ,<sup>11,12</sup> although a finite- $T$  transition was discussed in previous mean-field studies.<sup>13,14</sup>

To stabilize a ferroelectric ordering [a stripe ordering in terms of pseudospins, shown in Fig. 1(d)], a further degeneracy-lifting perturbation must be included. In the present study, we consider an intermolecular coupling originating from the distortion by forming C=C double bonds. A C=C double bond induces a trapezoid-type distortion of C<sub>4</sub> square, and favors a ferrotype alignment of the molecules since a short C=C bond tends to elongate the neighboring parallel C=C bonds in the adjacent molecules. The intermolecular correlation is incorporated by a third-neighbor ferromagnetic interaction  $J_3$  [Fig. 1(b)].  $J_3$  lifts the remaining degeneracy and selects the ferroelectrically ordered state.

By summarizing the above argument, our model is given by the following Hamiltonian:

$$\mathcal{H} = J_1 \sum_{\langle i,j \rangle} \sigma_i^z \sigma_j^z + J_2 \sum_{[i,j]} \sigma_i^z \sigma_j^z - J_3 \sum_{\{i,j\}} \sigma_i^z \sigma_j^z + \Gamma \sum_i \sigma_i^x, \quad (1)$$

where  $\sigma_i^\alpha$  is the  $\alpha$  component of the Pauli matrix, representing the pseudospin operator at site  $i$ ;  $J_1, J_2 > 0, J_3 \geq 0$ , and the first, second, and third sums are taken between the nearest, second (crisscrossing), and third neighbors on the checkerboard lattice, as shown in Fig. 1(b). Here, the last term with the transverse field  $\Gamma$  is introduced to represent the quantum tunneling of protons. We take  $J_1 = 1$  as the energy unit and focus on the case with  $J_2 = 2$ . The results are qualitatively the same for  $J_2 > J_1$ . We analyze the 2D model by changing  $J_3$ ,  $\Gamma$ , and  $T$  to clarify the nature of in-plane ferroelectricity in H<sub>2</sub>SQ; the effect of the interplane coupling will be mentioned later.

### B. Quantum Monte Carlo method

To investigate the thermodynamics of the model given by Eq. (1), we employ a recently developed continuous-time QMC method with a cluster update in the imaginary-time direction.<sup>20</sup> In order to overcome the slow relaxation in the present frustrated system, we use the replica exchange method<sup>21</sup> and the loop-flip update algorithm.<sup>22</sup> In the replica exchange, the replicas are chosen along the constant  $\Gamma/T$  lines since the Boltzmann weight strongly depends on the numbers of domain walls along the imaginary-time direction, which are proportional to  $\Gamma/T$ . For the loop-flip algorithm, we applied two variants of the original algorithm. One is the original algorithm that forms a loop by connecting up spins and down spins alternatively while treating the  $J_1$  and  $J_2$  bonds equivalently. The other one is the diagonal flipping process; a diagonal chain of spins connected by  $J_2$  is flipped at once. The system sizes are taken from  $L = 24$  to  $36$  ( $N = 4L^2$ ) under periodic boundary conditions. Typically, MC measurements are performed for 100 000 samplings after 30 000 initial thermalizations. Results are divided into six bins to estimate statistical errors by the variance among the bins.

### C. Physical quantities

To distinguish the long-range order and “ice-rule”-type local correlations, we calculate the macroscopic polarization

$P$  and local correlation parameter  $\rho$ .  $P$  is calculated as

$$P = \frac{1}{N} [S(0, \pi)^2 + S(\pi, 0)^2]^{1/2} \quad (2)$$

via the spin structure factor

$$S(\mathbf{k}) = \frac{1}{N} \sum_{i,j} \sigma_i^z \sigma_j^z \exp(-i\mathbf{k} \cdot \mathbf{r}_{ij}), \quad (3)$$

which detects the stripe-type ordering in Fig. 1(d). The critical temperature is determined by the Binder analysis<sup>23</sup> using the Binder parameter for  $P$ ,

$$g_P = \frac{1}{2} \left( 3 - \frac{\langle P^4 \rangle}{\langle P^2 \rangle^2} \right). \quad (4)$$

On the other hand,  $\rho$  detects the fourfold-degenerate stable configurations in each plaquette by

$$\rho = \frac{2}{N} \sum_p f(p), \quad (5)$$

where the sum  $p$  runs over all the crisscrossing plaquettes, and  $f(p)$  is a function giving 1 for the fourfold stable states and otherwise  $-1/3$  in  $p$ th plaquette:  $\rho \rightarrow 0$  when the spins are completely disordered, and  $\rho \rightarrow 1$  when all the plaquettes are in the fourfold stable states. Note that  $\rho$  is not an order parameter but characterizes a crossover associated with the formation of molecular polarizations as demonstrated below. We also measure the corresponding susceptibilities,  $\chi_P$  and  $\chi_\rho$ , from the fluctuations of  $P$  and  $\rho$  as

$$\chi_P = \frac{N}{T} (\langle P^2 \rangle - \langle P \rangle^2), \quad (6)$$

$$\chi_\rho = \frac{N}{T} (\langle \rho^2 \rangle - \langle \rho \rangle^2), \quad (7)$$

respectively. The specific heat is calculated by

$$C = \frac{1}{NT^2} (\langle \mathcal{H}^2 \rangle - \langle \mathcal{H} \rangle^2). \quad (8)$$

### III. RESULTS

#### A. Locally correlated liquidlike state

Figure 2 shows QMC results along the  $\Gamma/T = \tan(\pi/6)$  axis at  $J_3 = 0.002$  and  $0.004$ . At the lowest  $T$ , the system shows a ferroelectric ordering with fully saturated polarization  $P$ , as shown in Figs. 2(a) and 2(e). With increasing  $T$  and  $\Gamma$ ,  $P$  steeply decreases and the corresponding susceptibility  $\chi_P$  shows a sharp peak that grows as  $N$  increases, indicating a phase transition into a paraelectric state. The critical temperature  $T_c$  is estimated from the crossing point of the Binder parameter of  $P$  given by Eq. (4), as shown in Figs. 2(d) and 2(h):  $T_c = 0.60(30)$  for  $J_3 = 0.002$  and  $T_c = 0.76(12)$  for  $J_3 = 0.004$ . On the other hand, the local correlation parameter  $\rho$  remains to be large even above  $T_c$  and gradually decreases for  $T \gtrsim 1.0$  [Figs. 2(b) and 2(f)]. Correspondingly, the specific heat  $C$  divided by  $T$  has a peak, as shown in Figs. 2(c) and 2(g). The susceptibility for  $\rho$ ,  $\chi_\rho$ , shows a broad peak at a higher  $T$ . These indicate that the system does not directly enter into a completely disordered state at  $T_c$  but exhibits an intermediate state in which molecular polarizations are retained; the system

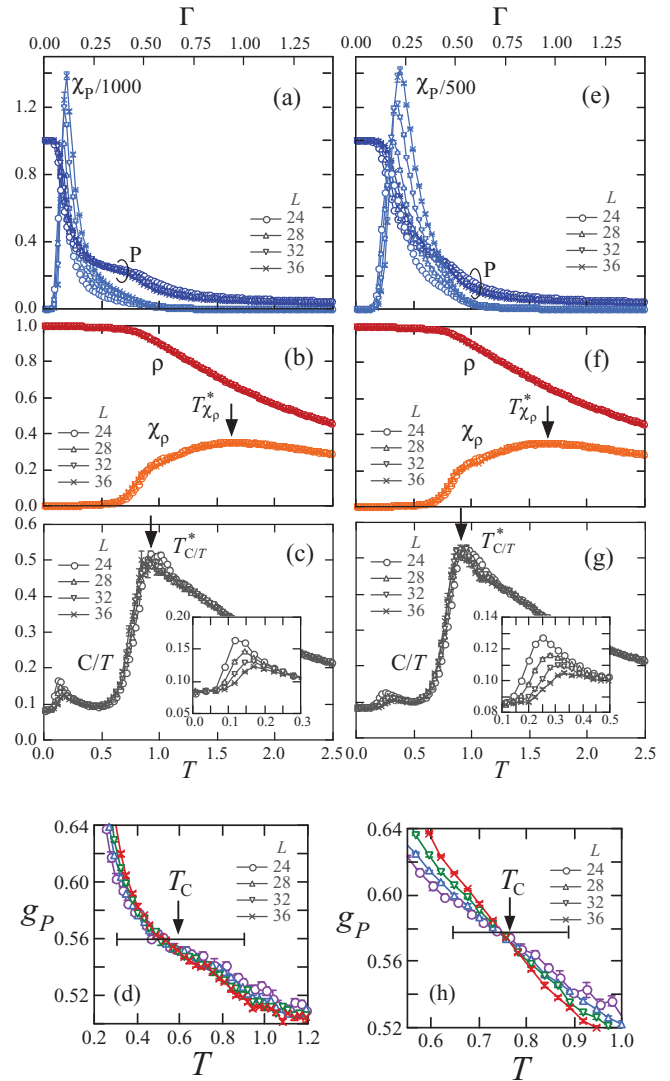


FIG. 2. (Color online) QMC results of (a),(e)  $P$  and  $\chi_P$  ( $\chi_P$  is divided by 1000 and 500, respectively); (b),(f)  $\rho$  and  $\chi_\rho$ ; and (c),(g)  $C/T$  for the system sizes  $N = 4L^2$  ranging from  $L = 24$  to  $36$ . The data are at (a)–(c)  $J_3 = 0.002$  and (e)–(g)  $J_3 = 0.004$ . (d) and (h) show the Binder parameter of  $P$  in the vicinity of  $T_c$  for  $J_3 = 0.002$  and  $0.004$ , respectively. Insets of (c),(g) show the low- $T$  behaviors of  $C/T$ . All the results are calculated at  $J_2 = 2$  along the axis with  $\Gamma/T = \tan(\pi/6)$ . See the text for details.

shows a crossover to a completely disordered paraelectric state characterized by the peak of  $C/T$  or  $\chi_\rho$  at  $T_{C/T}^*$  or  $T_{\chi_\rho}^*$ . The intermediate state is a liquidlike paraelectric state originating from the ice-rule-type local correlations.

In the ferroelectric phase transition and crossover to liquidlike phase, most of the entropy is released at the crossover by forming the ice-rule-type manifold. As shown in Figs. 2(c) and 2(g),  $C/T$  sharply decreases with the saturation of  $\rho$ , and the peak associated with the phase transition at a lower  $T$  is very small. In fact, as shown in the insets, the intensity of the small peak decreases as  $N$  increases, while the peak position approaches  $T_c$ . This suggests that the entropy associated with the phase transition becomes vanishingly small in the thermodynamic limit. The peculiar behavior is understood by considering the quasimacroscopic degeneracy

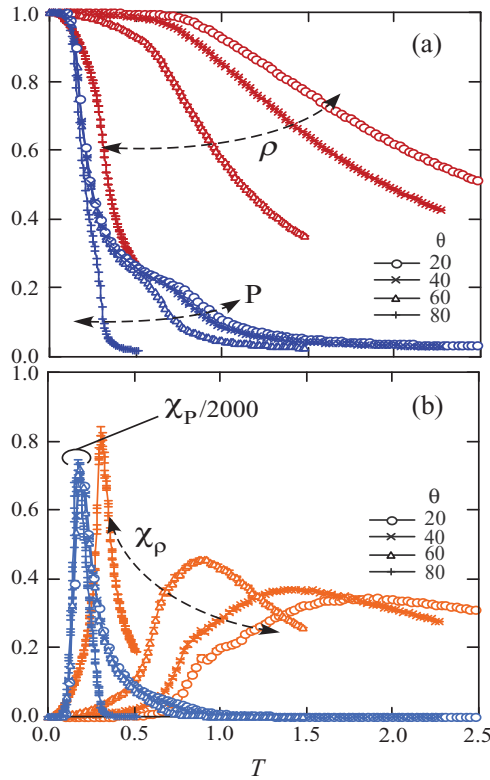


FIG. 3. (Color online)  $T$  dependences of (a)  $P$  and  $\rho$ , and (b)  $\chi_P/2000$  and  $\chi_\rho$ , measured along various  $\Gamma/T$ .  $\Gamma/T$  is parametrized by  $\theta$  (degree) with  $\Gamma/T = \tan\theta$ . All the results are calculated at  $J_2 = 2$  and  $J_3 = 0.002$  for  $N = 4 \times 36^2$  sites.

in the ice-rule-type manifold where the remaining entropy is in the order of  $\sqrt{N}$ , not  $N$ .<sup>12</sup>

The intermediate liquidlike state is widely observed while changing  $\Gamma/T$ . Figure 3 shows  $P$ ,  $\rho$ , and their susceptibilities along the various  $\Gamma/T$  axes. As indicated by a decrease of  $\rho$  and a broad peak of  $\chi_\rho$ , the crossover temperature  $T^*$  largely decreases with increasing  $\Gamma$ , while the data of  $P$  and  $\chi_P$  show that  $T_c$  does not decrease so rapidly. However, there is always a window of the intermediate state with well-developed local correlations and suppressed global order even for large  $\theta$ .

### B. Phase diagrams

The phase diagrams for  $\Gamma$ ,  $T$ , and  $J_3$  are summarized in Fig. 4. ( $T_c, \Gamma_c$ ) are estimated by the Binder analysis of  $P$ , and ( $T^*, \Gamma^*$ ) are identified by a peak of  $\chi_\rho$  or  $C/T$ . In the case of  $J_3 = 0$ , the system exhibits only the crossover into the liquidlike state with quasimacroscopic degeneracy [the region below  $T_{\chi_\rho}^*$ ; see Figs. 2(b) and 2(f)], and remains paraelectric down to the lowest  $T$  calculated. One might expect a quantum order by disorder as predicted for the case of  $J_1 = J_2$ ,<sup>24</sup> but it will be limited to the very low  $T$  region, if any, and is beyond the scope of the present study. With  $J_3$  switched on, the degeneracy is lifted and the ferroelectrically ordered phase emerges inside the liquidlike state. The ordered state rapidly extends with increasing  $J_3$ , but a sequential change of the three different regimes is clearly observed in the region where  $J_3$

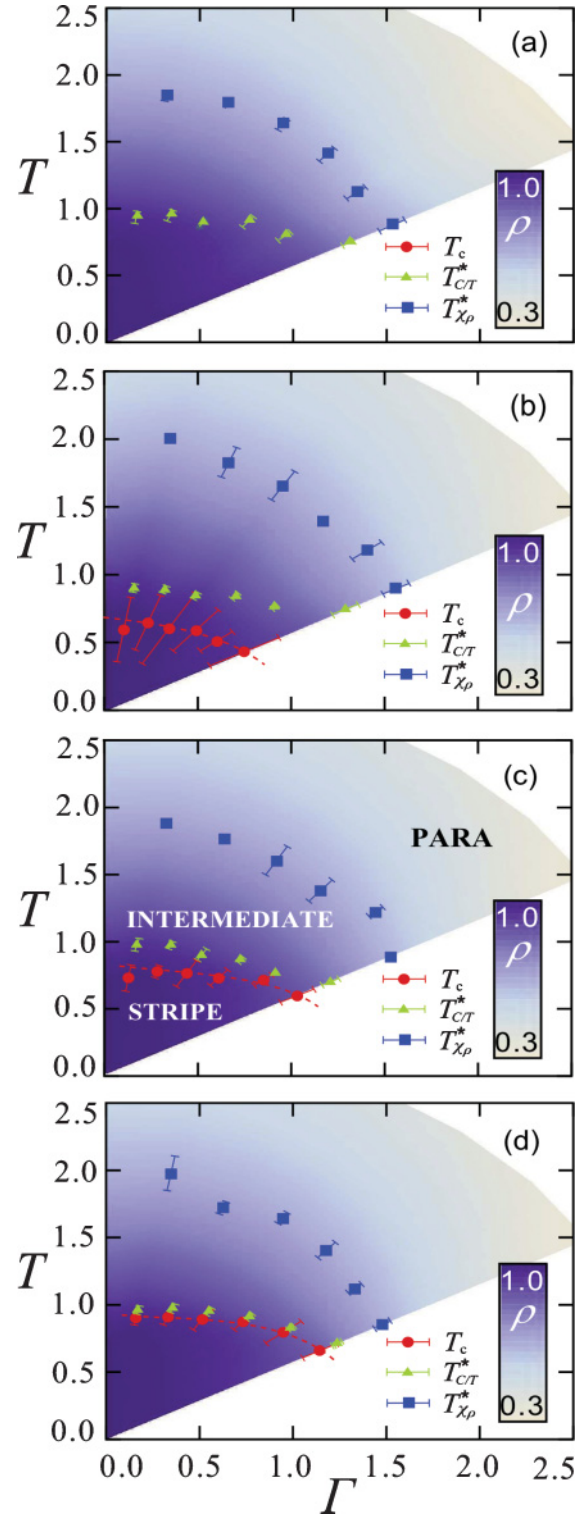


FIG. 4. (Color online) Phase diagrams obtained for varying  $J_3$ . Each diagram for (a)–(d) corresponds to  $J_3 = 0, 0.002, 0.004$ , and  $0.008$ , respectively. The solid circles show  $T_c$  obtained by the Binder parameter of  $P$  and triangular (square) points are  $T^*$  evaluated from  $C/T$  ( $\chi_\rho$ ). The dotted line shows the phase boundary of the ordered state and the paraelectric state, and the intermediate state is assigned as the region between  $T_{\chi_\rho}^*$  and  $T_c$ . The gradation shows the intensity of  $\rho$ .

is sufficiently small. With further increasing  $J_3$ ,  $T_c$  exceeds  $T^*$  and the intermediate liquidlike state is taken over by the long-range-ordered state.

A remarkable point of the phase diagram is the rapid growth of  $T_c$  with  $J_3$ , which is more than 100 times larger than  $J_2$ . This colossal enhancement of  $T_c$  is also ascribed to the peculiar nature of the intermediate state with quasimacroscopic degeneracy; the spatial correlations are strongly enhanced along the diagonal chains. This strong correlation reinforces the effect of  $J_3$  as  $J_2$  and  $J_3$  are not frustrated, and the system becomes extremely sensitive to the degeneracy-lifting perturbation  $J_3$ . Another point is the fate of the intermediate state at low temperatures. Since the QMC simulation becomes harder for larger  $\Gamma/T$ , it is difficult to conclude whether the intermediate state remains at low temperatures. Nonetheless, we expect a finite window down to low  $T$  for small  $J_3$  from the systematic change of the phase diagram shown in Fig. 4.

#### IV. DISCUSSIONS

Comparing with experiments, we successfully identify the liquidlike state with well-developed molecular polarizations, which might account for the peculiar intermediate state in experiments.<sup>10</sup> Our results suggest that the intriguing physics related with the ice-rule-type degeneracy is involved within the 2D layers of  $\text{H}_2\text{SQ}$  crystal. We note, however, that the qualitative shape of the phase diagram appears to be different; in experiments, both  $T_c$  and  $T^*$  decrease almost linearly in applied pressure and their difference is almost independent of pressure. This can be ascribed to the parametrization of the realistic situation, i.e., how the model parameters change under pressure. The first-principles calculations may help further quantitative studies.<sup>25</sup> Another possible origin of the discrepancy is an ambiguity in assigning  $T^*$ ; in general, the crossover boundary depends on how to define or detect it. With regard to the nature of the phase transition, our results indicate that it is second order and the associated anomaly of the specific heat is vanishingly small. This apparent contradiction with experiments<sup>26–28</sup> might be reconciled by considering the interlayer coupling or more complicated couplings to lattice distortions, which are neglected in our model.<sup>16,29,30</sup>

Comparing with the previous theoretical research, our results are obtained by seriously including both geometrical frustration and quantum fluctuation, which were not fully taken into account in previous studies. For instance, in the absence of  $J_3$ , our result shows no phase transition as expected in the frustrated situation, in contrast to the previous research in which a finite-temperature phase transition was predicted because of the mean-field-type treatment. Furthermore, our result clearly indicated the existence of the liquidlike state as well as several significant consequences of the local correlation on the thermodynamic properties. In particular, the absence

of an anomaly in the specific heat at  $T_c$  and the strong enhancement of  $T_c$  by  $J_3$  are revealed by our calculations. On the other hand, as mentioned above, our result also showed a continuous transition as in many previous theoretical studies using pseudospin or an equivalent approach. This suggests that an extension of the model is necessary to account for the first-order transition in experiments.

#### V. SUMMARY

To summarize, we have investigated the geometrically frustrated transverse-field Ising model as an effective model for squaric acid crystals. Through unbiased QMC simulations we have identified an intermediate liquidlike state between the ferroelectrically ordered state and the completely disordered paraelectric state, in which molecular polarizations are well preserved but they are globally disordered due to the frustration. Furthermore, we found that the emergence of a locally correlated state significantly affects the thermodynamic behavior of this system. In particular, we unveiled the vanishingly small anomaly in the specific heat at the transition point and the colossal enhancement of  $T_c$  by the degeneracy-lifting perturbation  $J_3$ . To the best of our knowledge, the emergence of such a state and the remarkable effects have never been reported in previous theories. The liquidlike state accounts for a peculiar intermediate paraelectric state observed under external pressure in the squaric acid crystal.

Although our results qualitatively reproduce the peculiar phase diagram of the squaric acid under pressure, the quantitative changes of the critical temperature and the crossover temperature are different from those in experiments. Further quantitative research is necessary. For example, a detailed experimental analysis of the structure under pressure will be quite important for a more quantitative comparison between experiment and theory. Moreover, the first-principles calculation will help to identify the model parameters and their changes under pressure more precisely. On the other hand, our result exhibits second-order phase transition, which is in contrast to the first-order transition observed experimentally. This might require a further extension of the model, for example, by including the interlayer coupling and complicated couplings to lattice distortions. Such an extension is left for future work.

#### ACKNOWLEDGMENTS

The authors thank Y. Tokura for fruitful discussions. H.I. and Y.M. thank T. Misawa, Y. Motoyama, H. Shinaoka, and M. Udagawa for helpful comments. This research was supported by KAKENHI (No. 19052008, No. 20740225, and No. 22540372), and Global COE Program “the Physical Sciences Frontier.”

<sup>1</sup>J. D. Bernal and R. H. Fowler, *J. Chem. Phys.* **1**, 515 (1933).

<sup>2</sup>L. Pauling, *J. Am. Chem. Soc.* **57**, 2680 (1935).

<sup>3</sup>J. C. Slater, *J. Chem. Phys.* **9**, 16 (1941).

<sup>4</sup>R. Blinc, *J. Phys. Chem. Solids* **13**, 204 (1960).

<sup>5</sup>P. G. de Gennes, *Solid State Commun.* **1**, 132 (1963).

<sup>6</sup>M. E. Lines and A. M. Glass, *Principles and Applications of Ferroelectrics and Related Materials* (Oxford University Press, New York, 1977).

- <sup>7</sup>S. Horiuchi and Y. Tokura, *Nat. Mater.* **7**, 357 (2008).
- <sup>8</sup>D. Semmingsen, *Acta Chem. Scand.* **27**, 3961 (1973).
- <sup>9</sup>E. J. Samuelsen and D. Semmingsen, *J. Phys. Chem. Solids* **38**, 1275 (1977).
- <sup>10</sup>Y. Moritomo, Y. Tokura, H. Takahashi, and N. Mōri, *Phys. Rev. Lett.* **67**, 2041 (1991).
- <sup>11</sup>U. Deininghaus, *Z. Phys. B* **45**, 71 (1981).
- <sup>12</sup>J. F. Stilck and S. R. Salinas, *J. Chem. Phys.* **75**, 1368 (1981).
- <sup>13</sup>V. I. Zinenko, *Phys. Status Solidi B* **78**, 721 (1976).
- <sup>14</sup>E. Matsushita, K. Yoshimitsu, and T. Matsubara, *Prog. Theor. Phys.* **64**, 1176 (1980).
- <sup>15</sup>B. K. Chaudhuri, P. K. Dey, and T. Matsuo, *Phys. Rev. B* **41**, 2479 (1990).
- <sup>16</sup>J. M. Wesselinowa, A. T. Apostolov, and M. S. Marinov, *J. Phys. Condens. Matter* **7**, 1701 (1995).
- <sup>17</sup>N. Dalal, A. Klymachyov, and A. Bussmann-Holder, *Phys. Rev. Lett.* **81**, 5924 (1998).
- <sup>18</sup>M. J. Harris, S. T. Bramwell, D. F. McMorrow, T. Zeiske, and K. W. Godfrey, *Phys. Rev. Lett.* **79**, 2554 (1997).
- <sup>19</sup>A. P. Ramirez *et al.*, *Nature (London)* **399**, 333 (1999).
- <sup>20</sup>T. Nakamura, *Phys. Rev. Lett.* **101**, 210602 (2008).
- <sup>21</sup>K. Hukushima and K. Nemoto, *J. Phys. Soc. Jpn.* **65**, 1604 (1996).
- <sup>22</sup>A. Rahman and F. H. Stillinger, *J. Chem. Phys.* **57**, 4009 (1972).
- <sup>23</sup>K. Binder, *Z. Phys. B* **43**, 119 (1981).
- <sup>24</sup>R. Moessner and S. L. Sondhi, *Phys. Rev. B* **63**, 224401 (2001).
- <sup>25</sup>C. Rovira, J. J. Novoa, and P. Ballone, *J. Chem. Phys.* **115**, 6406 (2001).
- <sup>26</sup>E. Barth, J. Helwig, H.-D. Maier, H. E. Muser, and J. Petersson, *Z. Phys. B* **34**, 393 (1979).
- <sup>27</sup>W. Kuhn, H.-D. Maier, and J. Petersson, *Solid State Commun.* **32**, 249 (1979).
- <sup>28</sup>M. Mehring and J. D. Becker, *Phys. Rev. Lett.* **47**, 366 (1981).
- <sup>29</sup>U. Deiningham and M. Mehring, *Solid State Commun.* **39**, 1257 (1981).
- <sup>30</sup>C. L. Wang, Z. K. Qin, and D. L. Lin, *Phys. Rev. B* **40**, 680 (1989).